Cellular and Molecular Life Sciences (2021) 78:2821–2838
https://doi.org/10.1007/s00018-020-03665-x

ORIGINAL ARTICLE

Wip1 controls the translocation of the chromosomal passenger complex to the central spindle for faithful mitotic exit

Xianghua Zhang[1] · Ji Eun Park[1] · Eun Ho Kim[2] · Jihee Hong[1] · Ki-Tae Hwang[3] · Young A. Kim[4] · Chang-Young Jang[1]

Received: 10 March 2020 / Revised: 12 August 2020 / Accepted: 5 October 2020 / Published online: 16 October 2020

Abstract

Dramatic cellular reorganization in mitosis critically depends on the timely and temporal phosphorylation of a broad range of proteins, which is mediated by the activation of the mitotic kinases and repression of counteracting phosphatases. The mitosis-to-interphase transition, which is termed mitotic exit, involves the removal of mitotic phosphorylation by protein phosphatases. Although protein phosphatase 1 (PP1) and protein phosphatase 2A (PP2A) drive this reversal in animal cells, the phosphatase network associated with ordered bulk dephosphorylation in mitotic exit is not fully understood. Here, we describe a new mitotic phosphatase relay in which Wip1/PPM1D phosphatase activity is essential for chromosomal passenger complex (CPC) translocation to the anaphase central spindle after release from the chromosome via PP1-mediated dephosphorylation of histone H3T3. Depletion of endogenous Wip1 and overexpression of the phosphatase-dead mutant disturbed CPC translocation to the central spindle, leading to failure of cytokinesis. While Wip1 was degraded in early mitosis, its levels recovered in anaphase and the protein functioned as a Cdk1-counteracting phosphatase at the anaphase central spindle and midbody. Mechanistically, Wip1 dephosphorylated Thr-59 in inner centromere protein (INCENP), which, subsequently bound to MKLP2 and recruited other components to the central spindle. Furthermore, Wip1 overexpression is associated with the overall survival rate of patients with breast cancer, suggesting that Wip1 not only functions as a weak oncogene in the DNA damage network but also as a tumor suppressor in mitotic exit. Altogether, our findings reveal that sequential dephosphorylation of mitotic phosphatases provides spatiotemporal regulation of mitotic exit to prevent tumor initiation and progression.

Keywords DNA damage response · Aurora B · Homeostasis · Checkpoint · MKLP1

Xianghua Zhang, Ji Eun Park and Eun Ho Kim contributed equally to this study.

Electronic supplementary material The online version of this article (https://doi.org/10.1007/s00018-020-03665-x) contains supplementary material, which is available to authorized users.

✉ Young A. Kim
pathgirl@daum.net

✉ Chang-Young Jang
cyjang@sookmyung.ac.kr

[1] Drug Information Research Institute, College of Pharmacy, Sookmyung Women's University, Seoul 04310, Republic of Korea

[2] Department of Biochemistry, School of Medicine, Catholic University of Daegu, Daegu 42472, Republic of Korea

[3] Department of Surgery, Seoul National University Boramae Medical Center, Seoul 07061, Republic of Korea

[4] Department of Pathology, Seoul National University Boramae Medical Center, Seoul 07061, Republic of Korea

Introduction

Entry into mitosis involves a comprehensive structural reorganization, including cell rounding and cortical stiffening via rearrangement of the cytoskeleton [1, 2], nuclear envelope breakdown [3, 4], chromosome condensation [5], and assembly of the mitotic spindle [6]. These structural changes depend on a spatially and temporally confined pattern of phosphorylation by the activation of diverse mitotic Ser/Thr protein kinases, most importantly cyclin-dependent kinase 1 (Cdk1) and numbers of the Aurora and Polo-like kinase (Plk) families [7], and by the inactivation of counteracting phosphatases [8–10]. Among the mitotic kinases, Cdk1 plays a dominant role because it orchestrates mitotic entry and progression until all sister chromatids have aligned at the mitotic equator [11–13]. Following chromosome segregation, cells break down the mitotic structures such as mitotic spindles and reassemble interphase structures including the

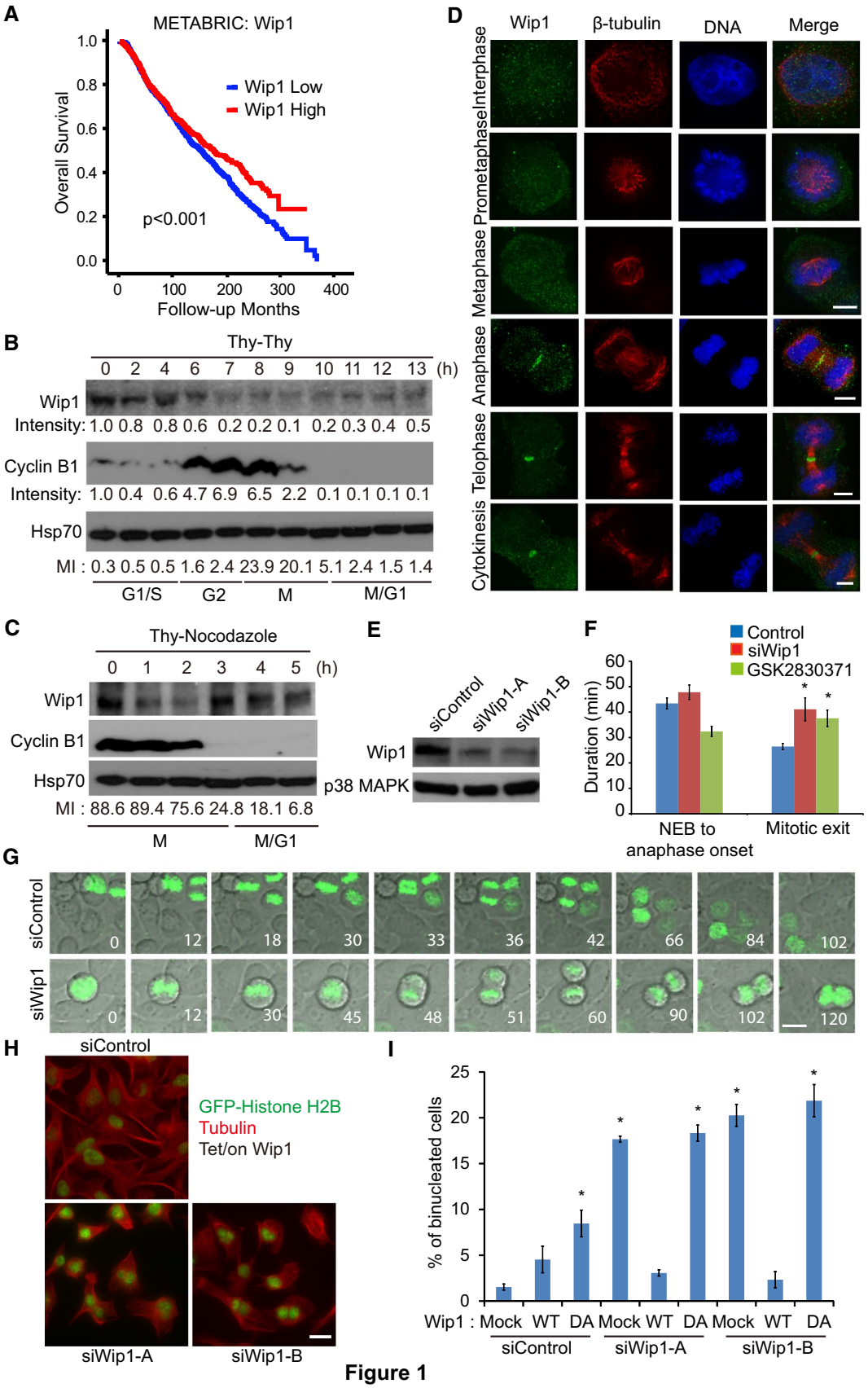
A
METABRIC: Wip1
Overall Survival
Wip1 Low
Wip1 High
p<0.001
Follow-up Months
B
Thy-Thy
0 2 4 6 7 8 9 10 11 12 13 (h)
Wip1
Intensity: 1.0 0.8 0.8 0.6 0.2 0.2 0.1 0.2 0.3 0.4 0.5
Cyclin B1
Intensity: 1.0 0.4 0.6 4.7 6.9 6.5 2.2 0.1 0.1 0.1 0.1
Hsp70
MI : 0.3 0.5 0.5 1.6 2.4 23.9 20.1 5.1 2.4 1.5 1.4
G1/S G2 M M/G1
C
Thy-Nocodazole
0 1 2 3 4 5 (h)
Wip1
Cyclin B1
Hsp70
MI : 88.6 89.4 75.6 24.8 18.1 6.8
M M/G1
D
Wip1 β-tubulin DNA Merge
Interphase
Prometaphase
Metaphase
Anaphase
Telophase
Cytokinesis
E
siControl siWip1-A siWip1-B
Wip1
p38 MAPK
F
Control
siWip1
GSK2830371
Duration (min)
NEB to anaphase onset
Mitotic exit
G
siControl
siWip1
0 12 18 30 33 36 42 66 84 102
0 12 30 45 48 51 60 90 102 120
H
siControl
GFP-Histone H2B
Tubulin
Tet/on Wip1
siWip1-A
siWip1-B
I
% of binucleated cells
Wip1 : Mock WT DA Mock WT DA Mock WT DA
siControl siWip1-A siWip1-B

Figure 1

◂**Fig. 1** Wip1 is an essential phosphatase for mitotic exit. **a** Overall survival curves of patients stratified according to the expression of the Wip1 mRNA in the METABRIC database. **b**, **c** HeLa cells were synchronized by a double thymidine block (**b**) or thymidine-nocodazole block (**c**), released into fresh media, and harvested at the indicated times. Cell lysates were analyzed via Western blotting with the indicated antibodies. Relative intensities of the bands were measured with image processing software (Image Studio ver5.0). The mitotic index (MI) was determined by fluorescence-activated cell sorting (FACS) with anti-MPM2 antibody staining. Hsp70 served as a loading control. **d** HeLa cells were fixed with MeOH and stained with the indicated antibodies. Images are maximum projections from z stacks of representative cells stained for Wip1 (green), β-tubulin or Plk1 (red), and DNA (blue). Scale bars, 5 μm. **e** HeLa cells were transfected with control (siControl) or Wip1-specific siRNAs (siWip1-A and siWip1-B) and harvested at 72 h after transfection. Lysates were analyzed by Western blotting with the indicated antibodies. **f**, **g** HeLa/GFP-histone H2B cells were treated with siWip1-A or the Wip1 inhibitor GSK2830371, and imaged for GFP-histone H2B using time-lapse microscopy starting at 60 h after transfection. Images were captured every 3 min to monitor mitotic progression. The duration from nuclear envelope breakdown (NEB) to chromosome segregation (NEB to anaphase onset) and from anaphase onset to chromosome decondensation (mitotic exit) were measured for control and Wip1-depleted cells ($n=40$ cells). Still frames from time-lapse movies of representative cells are shown in (**g**). Scale bar, 10 μm. **h**, **i** HeLa/GFP-histone H2B cells stably transfected with tetracycline-inducible WT Wip1 or the DA mutant were transfected with siControl or siWip1. The cells were treated with doxycycline to induce Wip1 protein expression at 48 h post-transfection and fixed with methanol. After staining with a β-tubulin antibody, binucleated cells were counted in three independent experiments ($n=500$ interphase cells for each quantification). Scale bar, 20 μm. Error bars, SEM. $^{*}p<0.01$ (two-tailed *t*-test)

nuclear envelope. Mitotic exit requires the reversal of mitotic phosphorylation, and a decrease in Cdk1 activity due to Cyclin B degradation concomitant with ordered bulk dephosphorylation of the substrates by mitotic exit phosphatases drives these processes in the eukaryotic cell cycle [14]. In budding yeast, the well-characterized dual-specificity phosphatase Cdc14 appears to dephosphorylate most of the mitotic regulators that were phosphorylated by Cdk1 during mitotic entry [15, 16]. While the vertebrate orthologues Cdc14A and Cdc14B may compensate for Cdc14 yeast phenotypes through functional conservation [17, 18], they are dispensable for mitotic exit in higher eukaryotes [19, 20]. Although phosphatases of the PP1 and PP2A families have come into focus as Cdk1-counteracting phosphatases in animal cells [10, 21], the identity of the phosphatases responsible for the temporal ordering of mitotic exit events is still debated.

Aurora B, one of the main regulators of mitotic exit, forms the chromosomal passenger complex (CPC) in conjunction with Survivin, inner centromere protein (INCENP), and Borealin [22, 23]. Dynamic translocation of the CPC during mitosis secures spatiotemporal phosphorylation of substrates that are associated with chromosome condensation, correct kinetochore-microtubule attachments, and cytokinesis [24]. At the entry of mitosis, the CPC is recruited to the chromosome arms and induces hypercondensation of mitotic chromosomes by phosphorylation of histone H3 Ser10 [25, 26]. During prometaphase, Survivin reads phosphorylated histone H3 Thr3 (H3T3) through a process mediated by Haspin and promotes the accumulation of the complex at the inner centromeres [27], where it controls activation of the spindle assembly checkpoint (SAC) to achieve spindle biorientation [28]. For mitotic exit, the complex dissociates from chromosomes via PP1-mediated H3T3 dephosphorylation and transfers to the central spindle via the interaction of INCENP and Aurora B with mitotic kinesin-like protein 2 (Mklp2) upon anaphase because the Cdk1-mediated inhibitory phosphorylation at Thr59 in INCENP is removed by mitotic exit phosphatases including PP2A [29–31]. Dephosphorylated INCENP also localizes to the equatorial cortex, where the CPC coordinates central spindle formation, cleavage furrow ingression, and abscission via the assembly of the cytokinetic machinery [32, 33].

Here, we show that Wip1/PPM1D drives CPC relocation by dephosphorylating of Thr59 in INCENP at the anaphase central spindle after CPC release from the chromosome via dephosphorylation of Thr3 in histone H3 by PP1. Because Wip1 localizes to the central spindle by interacting with MKLP2 and dephosphorylates INCENP around the central spindle, its depletion induces a delay in mitotic exit and eventually results in binuclear cells. Thus, coordination among the PP1, PP2A, and Wip1 dephosphorylation cascades plays a critical role during determining the cellular localization of the CPC in mitotic exit and secures precise cytokinesis.

Results

Wip1 localizes to the central spindle and midbody for faithful mitotic exit

Wip1 was first identified as a p53 target gene induced by various types of DNA damage and maintains homeostatic balance by dephosphorylating proteins involved in DNA damage processing such as ATM, Chk1, Chk2, p53, γ-H2AX, XPA, and XPC after repairing damaged DNA [34, 35]. In this regard, Wip1 functions as an oncogene by suppressing DNA repair and the concomitant development of new mutations during tumorigenesis. Consistent with this evidence, the Wip1 gene is amplified and overexpressed in numerous tumors, including breast cancer [36, 37]. To delineate the role of Wip1 as an oncogene in tumor progression, we sought to analyze the mRNA expression patterns of phosphatases, including Wip1, PP1, PP2A, and PP2B and their correlations with clinical factors in patients with breast cancer based on the data obtained from the METABRIC (Molecular Taxonomy of Breast Cancer International

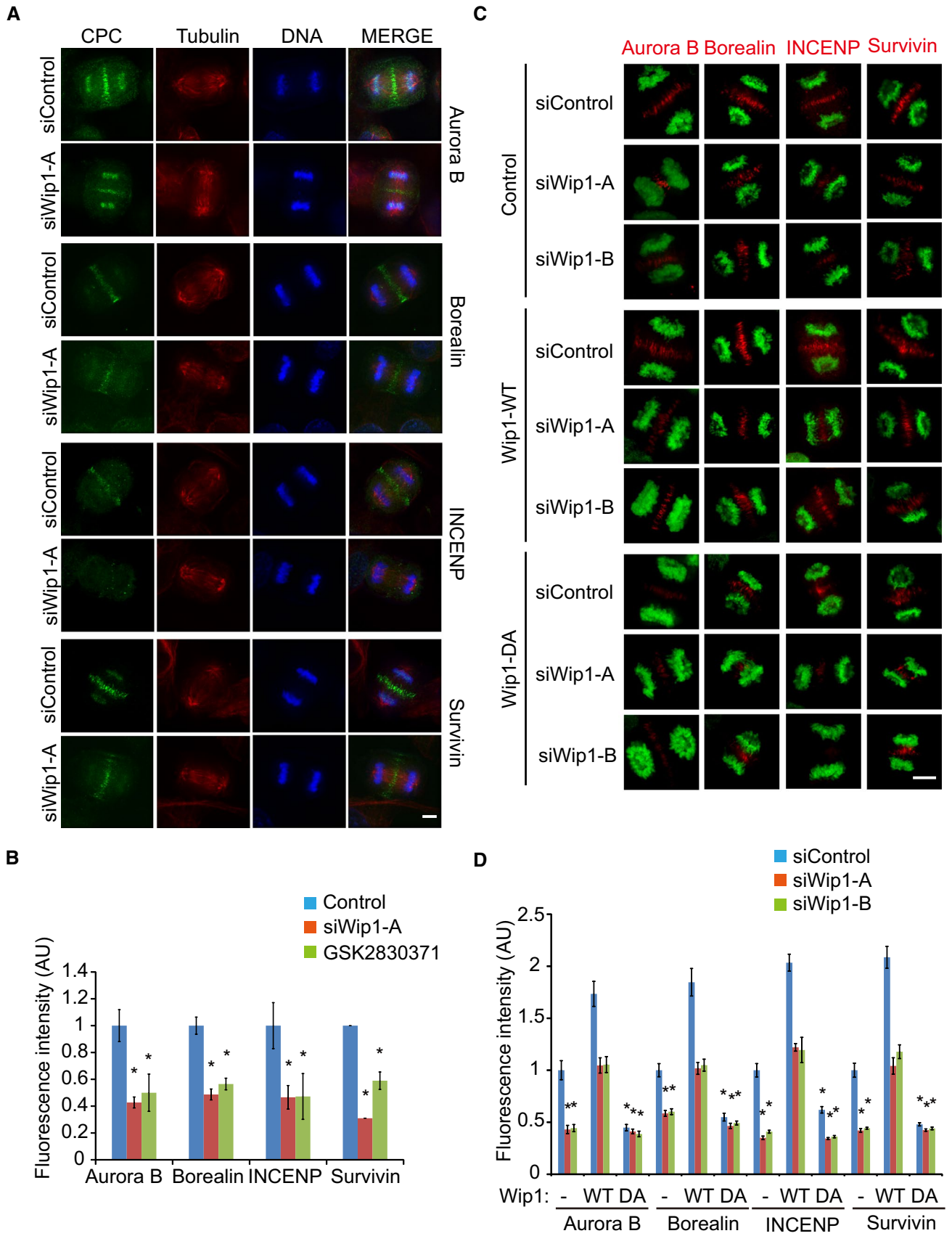
A
CPC
Tubulin
DNA
MERGE
siControl
siWip1-A
Aurora B
Borealin
INCENP
Survivin
C
Aurora B
Borealin
INCENP
Survivin
Control
Wip1-WT
Wip1-DA
siControl
siWip1-A
siWip1-B
B
Control
siWip1-A
GSK2830371
Fluorescence intensity (AU)
1.4
1.2
1
0.8
0.6
0.4
0.2
0
Aurora B
Borealin
INCENP
Survivin
D
siControl
siWip1-A
siWip1-B
Fluorescence intensity (AU)
2.5
2
1.5
1
0.5
0
Wip1: - WT DA - WT DA - WT DA - WT DA
Aurora B
Borealin
INCENP
Survivin

◂**Fig. 2** Wip1 is required for CPC translocation to the central spindle in anaphase. **a**, **b** After treatment with siWip1-A for 72 h or the Wip1 inhibitor for 24 h, HeLa cells were stained with antibodies against CPC components, and the intensity was determined from 30 anaphase cells in three independent experiments. **c**, **d** Forty-eight hours after siRNA transfection, HeLa/GFP-histone H2B cells stably transfected with tetracycline-inducible WT Wip1 or the DA mutant were treated with doxycycline for 24 h to induce Wip1 protein expression. The cells were stained with a β-tubulin antibody and the intensity of CPC components was determined from 30 anaphase cells in three independent experiments. Scale bars, 5 μm. Error bars, SEM. $*p < 0.01$ (two-tailed *t*-test)

Consortium) database. Although PP2B, but not PP1 and PP2A, correlated with the overall survival rate among these proteins, Wip1 showed the strongest correlation with the overall survival rate of patients with breast cancer (Fig. 1a, Supplementary Fig. 1a). Strikingly, the high-Wip1 group exhibited a higher overall survival rate than the low-Wip1 group, which cannot be explained by the oncogenic potential of Wip1. To interpret this unexpected result, we focused on the mitotic function of Wip1, whose phosphatase activity has reportedly been necessary for normal mitotic progression [38, 39]. Although Wip1 expression decreased in early mitosis, the levels of Wip1 recovered during mitotic exit in the synchronous cell cycle progression of HeLa cells (Fig. 1b, c). Interestingly, Wip1 showed a mutually exclusive expression pattern with Cyclin B, suggesting that Wip1 appears to act as a Cdk1-counteracting phosphatase after degradation of Cyclin B and concomitant inactivation of Cdk1 during mitotic exit. We next determined the cellular localization of endogenous Wip1 throughout the cell cycle and found that recovered Wip1 was concentrated in the central spindle and midbody during mitotic exit (Fig. 1d). This localization contrasts with other mitotic phosphatases, such as PP1, PP2A, and PP2B, which appear in the centrosome, mitotic spindle, and telophase microtubules, respectively [40, 41] (Supplementary Fig. 1b–d). Therefore, Wip1 is the mitotic phosphatase that localizes to the mitotic structure for cytokinesis (Supplementary Fig. 2a). Consistent with previous data, Wip1 depletion by a siRNA or inhibition by an inhibitor caused a delay in mitotic exit and increased the numbers of anaphase cells and telophase cells (Fig. 1e, Supplementary Fig. 2b–d). To determine the function of Wip1 in cytokinesis, we generated HeLa cells stably expressing GFP-histone H2A for live cell imaging and found that the depletion of Wip1 resulted in a delay in mitotic exit and the formation of binucleated cells (Fig. 1f, g; Movie 1 and 2). Similar mitotic defects were observed in Wip1 inhibitor-treated HeLa cells (Fig. 1f, Supplementary Fig. 1e) and non-cancerous RPE1 cells (Supplementary Fig. 2f). To further confirm whether phosphatase activity is required for Wip1 function in mitotic exit, we took advantage of Wip1 inducible HeLa/GFP-H2B cells and found that wild type (WT) and a phosphatase-dead (DA) mutant [42, 43] localized to the anaphase central spindle (Supplementary Fig. 3a, b). Indeed, HeLa/GFP-H2B cells expressing WT Wip1 showed a reduction in the number of binucleated cells caused by Wip1 depletion with a siRNA targeting the untranslated region of the endogenous Wip1 gene, whereas HeLa/GFP-H2B cells expressing the DA mutant showed an increase in the number of binucleated cells by the DA itself and did not rescue Wip1 depletion (Fig. 1h, i). Thus, we conclude that Wip1 localizes to the central spindle and midbody upon mitotic exit and fulfills a crucial role at the end of mitosis as a mitotic exit phosphatase.

Wip1 mediates CPC translocation to the central spindle in anaphase

To elucidate the molecular function of Wip1 in cytokinesis, we searched for Wip1-interacting proteins by performing immunoprecipitation with mass spectrometry and obtained Aurora B as an interacting partner (Supplementary Fig. 3c, d). Immunoprecipitation assays indicated that Wip1 coprecipitated with Aurora B, Borealin, INCENP, and Survivin because Aurora B is a catalytic subunit of the CPC (Supplementary Fig. 3e). Although the levels of CPC components were not decreased (Supplementary Fig. 3f), the signals of CPC components at the central spindle were diminished and dispersed in Wip1-depleted or Wip1-inhibited cells (Fig. 2a, b, Supplementary Fig. 4f). Consistent with this finding, CPC components were decreased in the karyotypically stable cell, RPE1, after the treatment of the Wip1 inhibitor (Supplementary Fig. 4b). Strikingly, the level of the CPC at the central spindle was substantially increased upon the overexpression of WT Wip1 and the translocation defect of the CPC in Wip1-depleted cells was significantly reversed by WT Wip1, but not by the DA mutant (Fig. 2c, d). Although CPC and Mklp2 are interdependent for their translocation to the central spindle during anaphase [30], the levels of Mklp2, but not Mklp1, were not decreased in Wip1-depleted cells (Fig. 3a, Supplementary Fig. 5a). Interestingly, treatment with the Aurora B inhibitor, Hesperadin, decreased the levels of Mklp2 at the central spindle in Wip1-depleted cells (Supplementary Fig. 5b), suggesting that the kinase activity of Aurora B is essential for the translocation of Mklp2 to the central spindle and the subsequent recruitment of CPC and Mklp1. To determine whether Mklp2 acts as a docking site for Wip1 at the central spindle, we analyzed anti-Wip1, anti-Mklp2, and anti-Myc immunoprecipitates and identified an interaction of Wip1 with Mklp2 (Fig. 3b, Supplementary Fig. 5c). Furthermore, overexpressed Wip1 WT did not localize to the central spindle in Mklp2-depleted cells (Fig. 3c–e), indicating that Wip1 binds to Mklp2 in the central spindle and recruits CPC and Mklp1. In contrast, Wip1-depleted cells did not show these defects in early mitosis (Supplementary Fig. 5d). Therefore, we conclude that

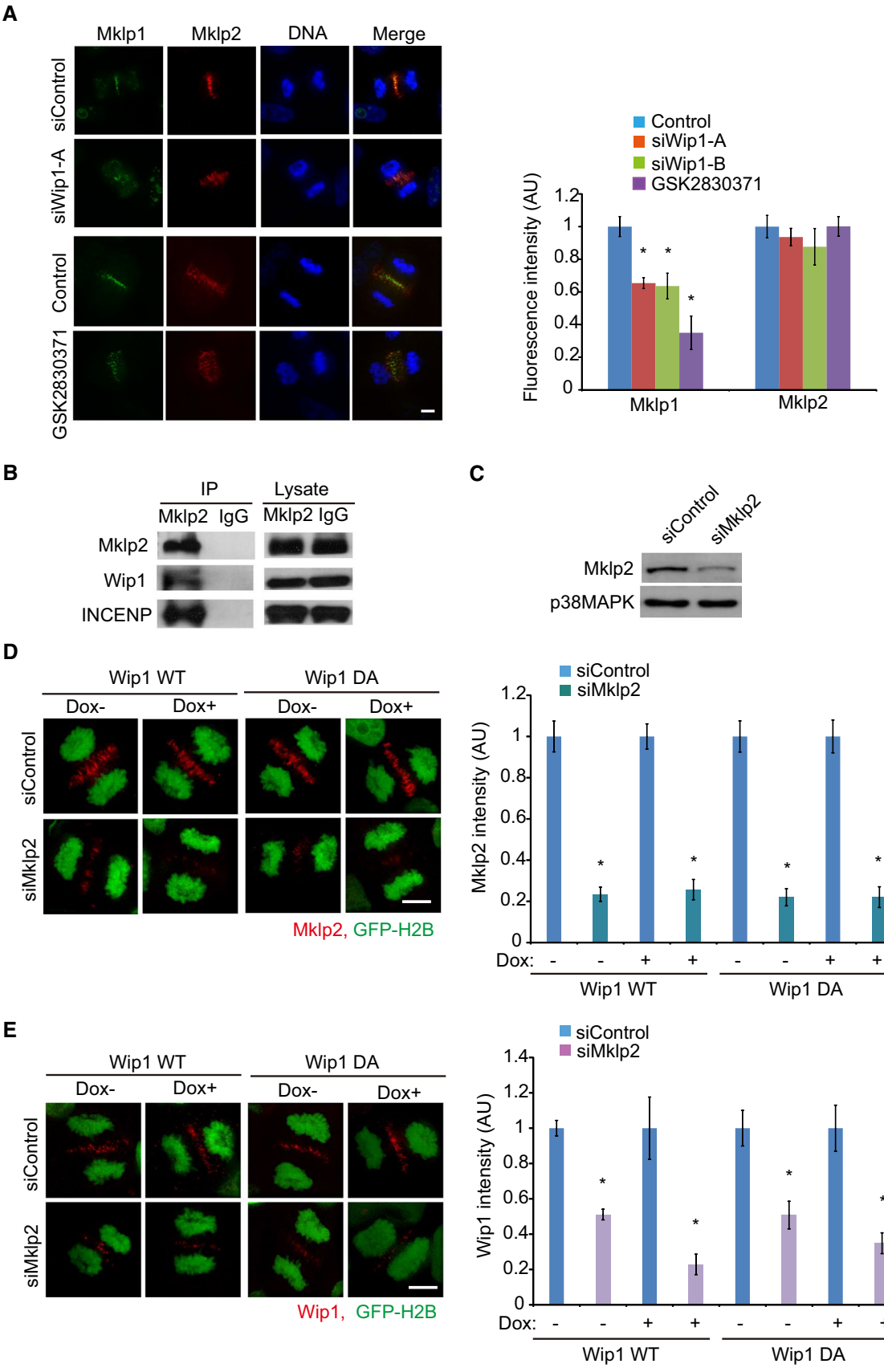
A
Mklp1
Mklp2
DNA
Merge
siControl
siWip1-A
Control
GSK2830371
Control
siWip1-A
siWip1-B
GSK2830371
Fluorescence intensity (AU)
1.2
1
0.8
0.6
0.4
0.2
0
Mklp1
Mklp2
B
IP
Lysate
Mklp2 IgG
Mklp2 IgG
Mklp2
Wip1
INCENP
C
siControl
siMklp2
Mklp2
p38MAPK
D
Wip1 WT
Wip1 DA
Dox-
Dox+
Dox-
Dox+
siControl
siMklp2
Mklp2, GFP-H2B
siControl
siMklp2
Mklp2 intensity (AU)
1.2
1
0.8
0.6
0.4
0.2
0
Dox: - - + + - - + +
Wip1 WT
Wip1 DA
E
Wip1 WT
Wip1 DA
Dox-
Dox+
Dox-
Dox+
siControl
siMklp2
Wip1, GFP-H2B
siControl
siMklp2
Wip1 intensity (AU)
1.4
1.2
1
0.8
0.6
0.4
0.2
0
Dox: - - + + - - + +
Wip1 WT
Wip1 DA

◂**Fig. 3** MKLP2 acts as a docking site for Wip1 at the central spindle in anaphase. **a** After treatment with siWip1-A or -B for 72 h or the Wip1 inhibitor for 24 h, HeLa cells were stained with the indicated antibodies and the intensity was determined from 30 anaphase cells in three independent experiments. **b** Lysates of HeLa cells were subjected to IP with an INCENP antibody followed by Western blotting. **c**–**e** Forty-eight hours after siRNA transfection, cells were prepared as described in Fig. 2c. The lysates were subjected to Western blotting (**c**). Cells were stained with an Mklp2 (**d**) or Wip1 antibody (**e**). The intensities of Mklp2 (**d**) and Wip1 (**e**) were determined from ten anaphase cells in three independent experiments. Scale bars, 5 μm. Error bars, SEM. *$p < 0.01$ (two-tailed *t*-test)

Wip1 plays a crucial role in CPC translocation to the central spindle for perfect cytokinesis.

Wip1 dephosphorylates Thr59 in INCENP during anaphase onset for CPC translocation

To determine the distinct function of Wip1 among the mitotic phosphatases, we examined mitotic defects such as chromosome alignment and binucleated cells in phosphatase inhibitor-treated cells. Although treatment with the PP2B inhibitor cyclosporin A caused chromosome alignment defects, the PP1/PP2A inhibitor calyculin A induced both chromosome alignment defects and the formation of binucleated cells (Fig. 4a, Supplementary Fig. 6a). We consistently found that the Wip1 inhibitor GSK2830371 promoted the formation of binucleated cells due to a cytokinesis failure, but not unaligned chromosomes. To analyze the spatiotemporal dynamics of cytokinesis after inhibition of mitotic phosphatases, we recorded data sets of mitotic chromosomes labeled with GFP-histone H2B. We followed the frames from the onset of anaphase to the completion of chromosome decondensation and confirmed similar cytokinesis failures such as the formation of binucleated cells and delay of mitotic exit, in cells treated with calyculin A and GSK2830371 (Fig. 4b, Supplementary Fig. 6b). Because calyculin A inhibits PP1 and PP2A in cells rescued by WT Wip1 overexpression (Fig. 4c), we took advantage of siPP1 and siPP2A siRNAs to examine the functional redundancy of Wip1 in cytokinesis. Intriguingly, overexpression of WT Wip1 reduced the number of binucleated cells in PP2A-depleted cells (Fig. 4d) but not in PP1-depleted cells (Fig. 4e). Because overexpression of WT Wip1 reverses the perturbation of CPC localization in PP2A-depleted cells (Fig. 4f), we reasoned that Wip1 and PP2A might mutually assist with the dephosphorylation of mitotic exit regulators as Cdk1-counteracting phosphatases. Therefore, we postulate that Wip1 plays a crucial role in mitotic exit in addition to its role in the homeostatic balance in the p53-dependent DNA damage response [43, 44].

To delineate the role of Wip1 in mitotic exit, we sought to identify the mitotic substrate during anaphase. Because PP1 and PP2A are involved in CPC translocation to the anaphase central spindle via dephosphorylation of Thr3 in histone H3 and Thr59 in INCENP [45–47], respectively, we analyzed the dephosphorylation of INCENP by using recombinant GST-Wip1 protein. We immunoprecipitated phosphorylated INCENP from HeLa S3 cells that were synchronized at prophase to perform an in vitro phosphatase assay and found that Wip1 dephosphorylated Thr59 of INCENP (Fig. 5a). In contrast, GST-Wip1 did not dephosphorylate Aurora B, which was immunoprecipitated from the same mitotic extract. In agreement with this finding, Wip1 dephosphorylated Thr59 of INCENP which was phosphorylated by recombinant Cdk1/Cyclin B in vitro (Fig. 5b), suggesting that INCENP is the physiological substrate of Wip1 in mitosis. These results raised the possibility that Thr59 in INCENP might be one of the target residues of Wip1 for faithful cytokinesis in mitotic exit. To explore this idea further, we sought to express an unphosphorylatable T59V or phosphomimetic T59E INCENP mutant in Wip1-depleted cells stably transfected with inducible WT Wip1 and observed translocation from the metaphase chromosome to the anaphase central spindle. Consistent with a previous study [31], WT and T59V mutant INCENP showed successful translocation to the central spindle at anaphase, in contrast to the INCENP T59E mutant (Fig. 5c, d). Interestingly, depletion of Wip1 perturbed the translocation of the INCENP WT but not the T59V mutant, indicating that Thr59 in INCENP is the major residue dephosphorylated by Wip1 during translocation to the central spindle. Consistent with this finding, the mislocalization of the INCENP WT, but not the INCENP T59E mutant, in Wip1-depleted cells was rescued by overexpression of WT Wip1 (Fig. 5c, d). Notably, double knockdown of Wip1 and PP2A showed a significant lack of translocation of INCENP WT compared with the depletion of Wip1 or PP2A alone (Fig. 5e). Strikingly, however, knockdown of Wip1 and/or PP2A did not affect the localization of INCENP T59V and T59E mutants at anaphase. Thus, we conclude that Wip1 and PP2A collaborate in the dephosphorylation of Thr59 in INCENP for CPC translocation to the anaphase central spindle.

Wip1 cooperates with PP1 for CPC translocation

Given that dephosphorylation of H3 at Thr3 by PP1 is involved in CPC translocation from the chromosome to the anaphase central spindle [47], we sought to investigate the relationship between PP1 and Wip1 in CPC translocation. Because the overexpression of WT Wip1 did not overcome the mislocation of the CPC induced by PP1 depletion (Supplementary Fig. 6c) and half of the T59E mutant was released from the chromosome to the cytosol in cells transfected with siControl (Fig. 6a), we speculated that the dephosphorylation of H3 Thr3ph is an initial step in CPC translocation during anaphase and Wip1 or PP2A

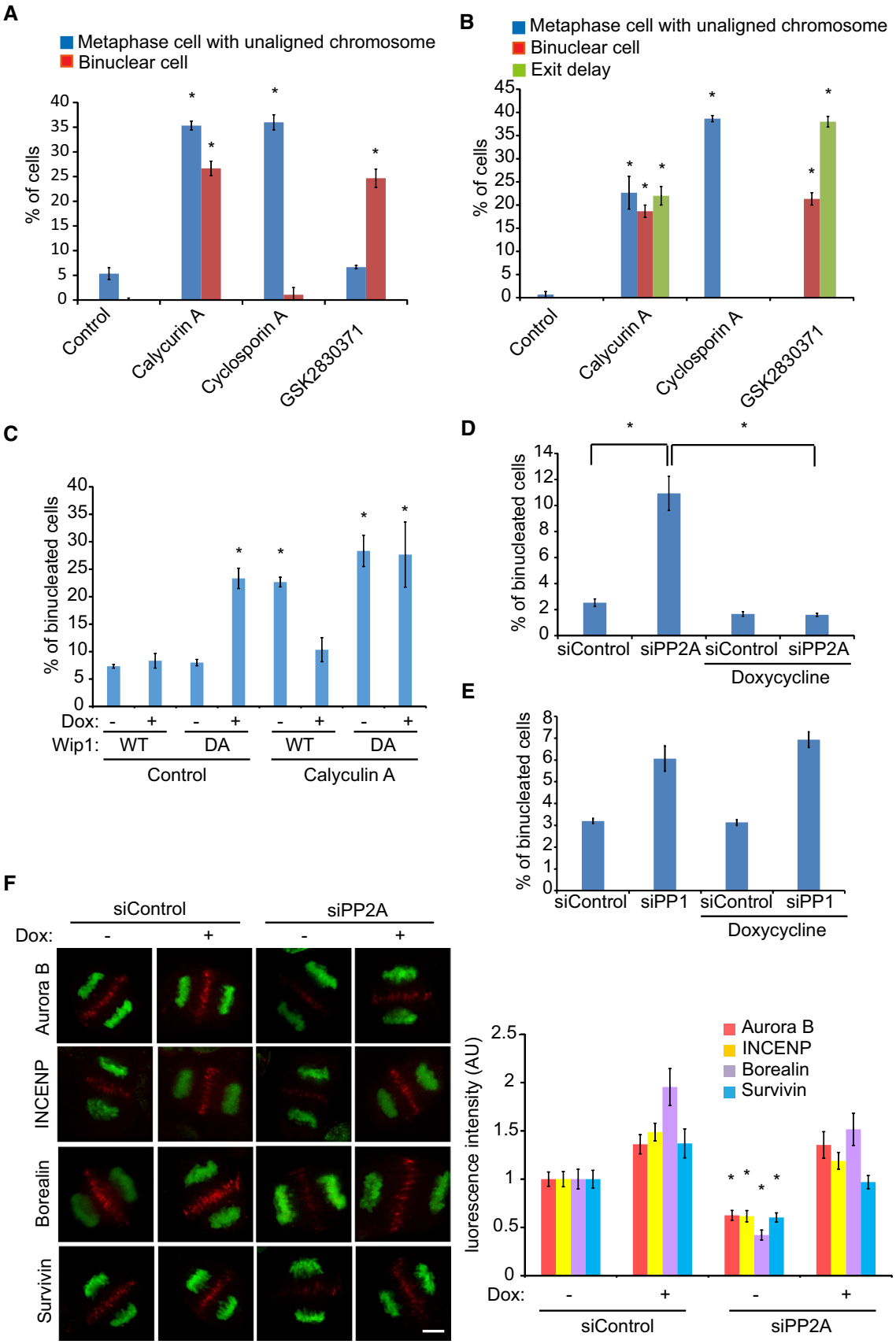
A
Metaphase cell with unaligned chromosome
Binuclear cell
% of cells
Control
Calycurin A
Cyclosporin A
GSK2830371
B
Metaphase cell with unaligned chromosome
Binuclear cell
Exit delay
% of cells
Control
Calycurin A
Cyclosporin A
GSK2830371
C
% of binucleated cells
Dox:
Wip1:
WT
DA
Control
Calyculin A
D
% of binucleated cells
siControl
siPP2A
Doxycycline
E
% of binucleated cells
siControl
siPP1
Doxycycline
F
siControl
siPP2A
Dox:
Aurora B
INCENP
Borealin
Survivin
luorescence intensity (AU)
Aurora B
INCENP
Borealin
Survivin

◂**Fig. 4** Wip1 compensates for the lack of PP2A during mitotic exit. **a** HeLa cells were treated with the PP1/PP2A inhibitor calyculin A for 5 h, the PP2B inhibitor cyclosporin A for 5 h, or the Wip1 inhibitor GSK2830371for 24 h. After staining with a β-tubulin antibody, binucleated cells and metaphase cells containing unaligned chromosomes were counted in three independent experiments ($n=500$ interphase cells for each quantification). **b** HeLa/GFP-histone H2B cells were treated with the indicated inhibitors and imaged for GFP-histone H2B by time-lapse microscopy. Images were captured every 3 min to monitor mitotic progression. Metaphase cells containing unaligned chromosomes, binucleated cells, and cytokinetic cells showing delayed mitotic exit (more than 40 min) were counted and plotted. **c** After inducing WT Wip1 or DA mutant protein, the cells were treated with calyculin A for 5 h and fixed with methanol. After staining with a β-tubulin antibody, binucleated cells were counted in three independent experiments ($n=500$ interphase cells for each quantification). **d**–**f** Forty-eight hours after siPP1 or siPP2A transfection, HeLa/GFP-histone H2B cells stably transfected with tetracycline-inducible WT Wip1 were treated with doxycycline for 24 h to induce Wip1 protein expression. After staining with a β-tubulin antibody, binucleated cells were counted in three independent experiments (**d**, **e**, $n=500$ interphase cells for each quantification). The cells were also stained with antibodies against CPC components, and the intensity was determined from 30 anaphase cells in three independent experiments (**f**). Scale bar, 5 μm. Error bars, SEM. $*p<0.01$ (two-tailed *t*-test)

dephosphorylates INCENP at Thr59 to promote CPC translocation after its release from the chromosome via PP1-mediated dephosphorylation of H3 at Thr3. Indeed, WT INCENP, the T59E mutant, and the T59V mutant did not release from chromosome in PP1-depleted cells (Fig. 6a).

Because Wip1 localized at the anaphase central spindle (Supplementary Fig. 2b) and PP2A accumulated at the mitotic spindle during metaphase and anaphase (Supplementary Fig. 1c), we focused on the localization of Wip1 to delineate the roles of Wip1 and PP2A in INCENP Thr59 dephosphorylation. Inadvertently, we found that both N-terminal Flag-tagged and C-terminal Flag-tagged Wip1 detached from the central spindle and diffused around the cytoplasm (Supplementary Fig. 7a). Because Flag-tagged Wip1 interacted with INCENP but not Mklp2 (Fig. 6b), we reasoned that the masking of the Mklp2 binding domain in Wip1 might be the reason for the mislocalization of Flag-tagged Wip1. Strikingly, Flag-tagged Wip1, which reportedly possessed normal phosphatase activity [39] and dephosphorylated etoposide-induced phosphorylated γ-H2AX (Fig. 6c) [43], failed to overcome cytokinetic failure caused by Wip1-depletion (Fig. 6d, e). This result raised the possibility that enrichment of Wip1 activity in the central spindle might be required for faithful cytokinesis in mitotic exit. Indeed, Wip1-depleted cells expressing Flag-tagged Wip1 still showed a reduction in CPC signals at the anaphase central spindle (Supplementary Fig. 7a), although Wip1-depleted cells expressing nontagged WT Wip1 showed a recovery of CPC levels at the central spindle (Fig. 2c, d). To dissect the role of PP2A and Wip1 in CPC translocation from the chromosome to the central spindle, we analyzed the localization of CPCs in anaphase after the depletion of PP1, PP2A, or Wip1 (Fig. 6f, g). We consistently found that most CPCs did not release from the chromosome in siPP1 cells. Interestingly, CPCs localized at the chromosome and central spindle in PP2A-depleted cells, suggesting that PP2A-mediated INCENP Thr59ph dephosphorylation facilitates detachment of CPCs from the chromosome in addition to PP1-mediated H3 Thr3ph dephosphorylation, but CPCs can be targeted to the central spindle without PP2A-mediated INCENP Thr59 dephosphorylation. In contrast, CPCs mainly dispersed in the cytosol and a few CPCs were located in the central spindle in Wip1-depleted cells, indicating that Wip1 dephosphorylates INCENP Thr59 at the anaphase central spindle after PP1-mediated release of CPCs from the mitotic chromosome. Although PP2A dephosphorylates INCENP Thr59ph, Wip1 is the major phosphatase against INCENP Thr59ph in cytokinesis, because overexpressed Wip1 rescued the generation of binucleated cells and mislocalization of CPC in siPP2A-transfected cells (Fig. 4c, e). Based on these results, we conclude that Wip1 dephosphorylates INCENP Thr59 at the chromosome and central spindle after the PP1-mediated release of CPC from the chromosome to target it to the central spindle (Fig. 7a).

Wip1 expression correlates with good patient prognosis in breast cancer

Despite the fact that Wip1 has been reported as an oncogene and is amplified in numerous tumors [37, 48], the high-Wip1 group showed a higher overall survival rate among patients with breast cancer (Fig. 1a), possibly because Wip1 has weak oncogenic potential in tumor progression by functioning as a negative regulator of DNA damage processing but suppresses tumor progression by ensuring faithful mitotic exit. In contrast, significant differences in PP2A levels were not observed between patients with breast cancer (Supplementary Fig. 1a), presumably because Wip1 compensates for a low level of PP2A as in PP2A-depleted cells (Fig. 5e). In this respect, we analyzed the correlation between the expression of Wip1 and PP2A in patients with breast cancer and observed a negative correlation (Supplementary Fig. 7b). Similar to Wip1 amplification in different intrinsic subtypes of breast cancer based on the PAM50 molecular profile [49], a high level of Wip1 expression was also related to a higher overall survival rate in patients with luminal A and luminal B but not in Her2 or basal subtypes of breast cancers (Fig. 7b). To confirm this pathophysiological data, we examined MCF-7 and T47D cells as luminal A breast cancer cell lines and MDA-MB-231 and HS578T cells as basal breast cancer cell lines. Consistent with the clinical data, MCF-7 and T47D cells showed a more significant increase in the number of binucleated cells than MDA-MB-231 and HS578T cells after Wip1 depletion (Fig. 7c, d,

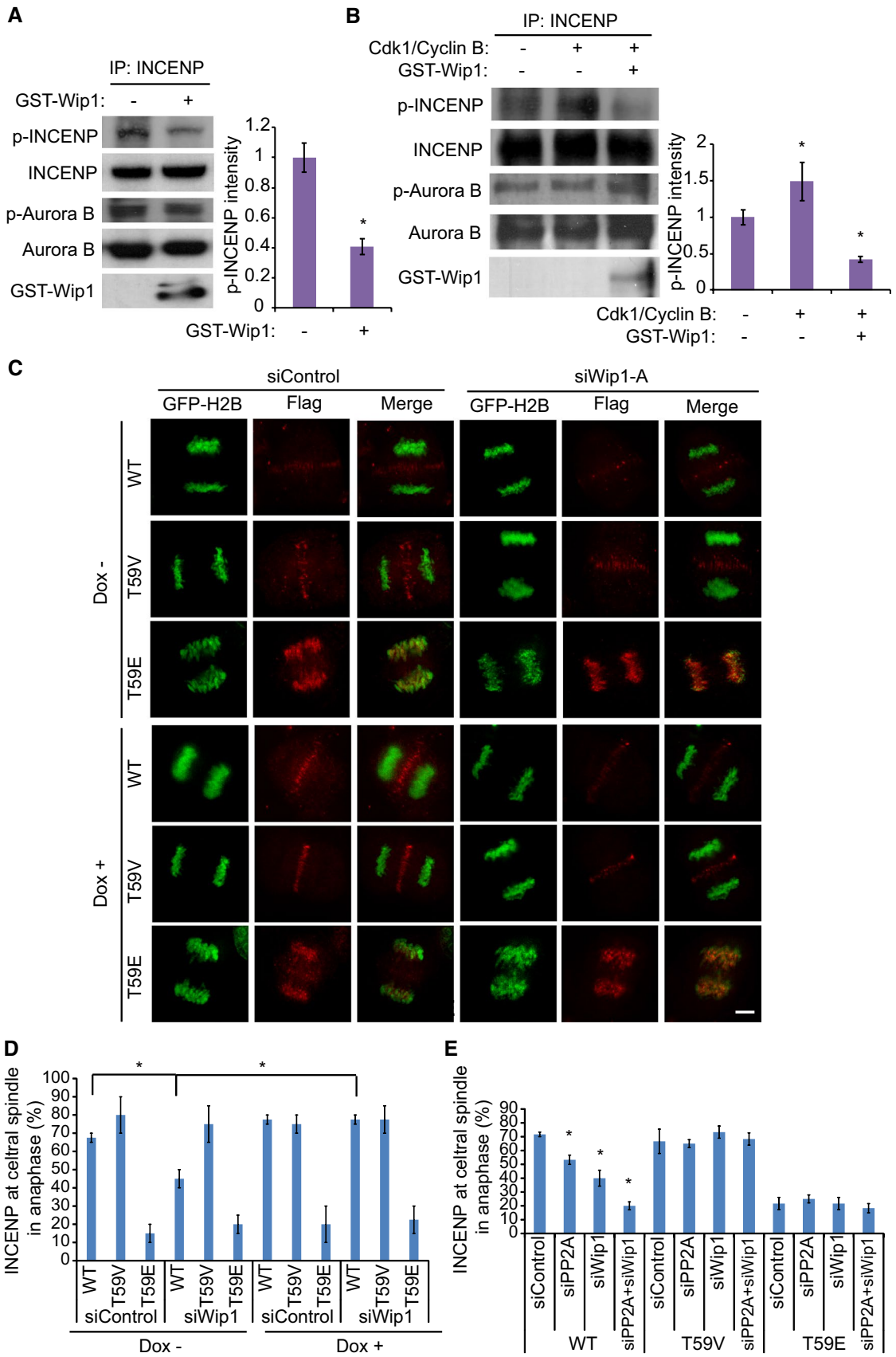
A
IP: INCENP
GST-Wip1: - +
p-INCENP
INCENP
p-Aurora B
Aurora B
GST-Wip1
p-INCENP intensity
GST-Wip1: - +
B
IP: INCENP
Cdk1/Cyclin B: - + +
GST-Wip1: - - +
p-INCENP
INCENP
p-Aurora B
Aurora B
GST-Wip1
p-INCENP intensity
Cdk1/Cyclin B: - + +
GST-Wip1: - - +
C
siControl
siWip1-A
GFP-H2B
Flag
Merge
Dox -
Dox +
WT
T59V
T59E
D
INCENP at celtral spindle in anaphase (%)
WT T59V T59E WT T59V T59E WT T59V T59E WT T59V T59E
siControl siWip1 siControl siWip1
Dox - Dox +
E
INCENP at celtral spindle in anaphase (%)
siControl siPP2A siWip1 siPP2A+siWip1 siControl siPP2A siWip1 siPP2A+siWip1 siControl siPP2A siWip1 siPP2A+siWip1
WT T59V T59E

◂**Fig. 5** Wip1 dephosphorylates Thr59 in INCENP for CPC translocation to the central spindle. **a** Thymidine-nocodazole arrested HeLa cells were treated with calyculin A for 5 h and then released into fresh media for 2 h. The lysates were incubated with Protein A agarose beads conjugated with antibodies against INCENP. Immunoprecipitates were incubated with GST-Wip1 for 30 min and analyzed by immunoblotting with antibodies as indicated. Relative intensities of the bands were measured from cells in three independent experiments using image processing software (Image Studio ver5.0). **b** HeLa cells were harvested under a non-synchronous condition. The lysates were incubated with Protein A agarose beads conjugated with antibody against INCENP. Immunoprecipitates were incubated with Cdk1/Cyclin B for 30 min. After washing with kinase buffer, phosphorylated immunoprecipitates were incubated with GST-Wip1 for 30 min and analyzed by immunoblotting with antibodies as indicated. Relative intensities of the bands were measured in cells from three independent experiments using image processing software (Image Studio ver5.0). **c**–**e** Forty-eight hours after siRNA transfection, HeLa/GFP-histone H2B cells were transfected with Flag-INCENP WT, the T59V mutant, or the T59E mutant. Twenty-eight hours after DNA transfection, the cells were stained with antibodies against Flag and the intensity was determined from 30 anaphase cells in three independent experiments. Scale bar, 5 μm. Error bars, SEM. $*p < 0.01$ (two-tailed *t*-test)

Supplementary Fig. 7c). Thus, we conclude that Wip1 plays a crucial role in tumor progression as a mitotic exit phosphatase in addition to its role in the DNA damage response network in a genotypic background-dependent manner.

Discussion

During mitosis, structural upheavals such as nuclear envelope breakdown, chromosome condensation, and cohesion, and spindle assembly are achieved through a combination of regulated proteolysis, phosphorylation, and dephosphorylation [10, 50, 51]. Massive phosphorylation is a landmark for mitotic entry and results in stoichiometric phosphorylation of proteins involved in the interphase-to-mitosis transition [52]. In addition to the activation of various mitotic kinases including Cdk1, Plk1, and Aurora kinases, the counteracting phosphatases are inactivated by inhibitors, covalent modifications, and subcellular targeting for bulk phosphorylation in mitotic entry [53]. Ensa/Arpp19 becomes an inhibitor of PP2A-B55 through phosphorylation by Greatwall kinase and reduces the concentration of Cdk1 needed to enter mitosis by blocking premature dephosphorylation of Cdk1 substrates [54]. In budding yeast, Zds1/Zds2 inhibits PP2A-B55 by retaining a pool of phosphatase in the cytoplasm to control mitotic entry [55]. Here, we show that Wip1 acts as a Cdk1-counteracting phosphatase in mitotic exit via dephosphorylation of INCENP and concomitant translocation of the CPC to the central spindle. Wip1 has recently been reported to be degraded by APC/C in early mitosis for normal mitotic progression, and overexpression of Wip1 causes a delay in the transition from metaphase to anaphase [38]. Furthermore, Wip1 is phosphorylated by Cdk1 during mitosis, leading to inhibition of its phosphatase activity [39]. Thus, the combined degradation and inhibition of Wip1 decrease the threshold of Cdk1 activity necessary for unperturbed mitotic progression until Cyclin B degradation and concomitant anaphase onset (Fig. 1b, c).

Because Wip1 acts as a negative regulator of several tumor suppressors that are implicated in the DNA damage response network including the p53 and p38 MAPK pathways, its overexpression increases genome instability by potentiating a negative feedback loop of the p53 response pathway and promotes breast cancer development [56]. Consistent with this information, DNA microarray analysis, and tissue microarray profiling showed that Wip1 is amplified and/or overexpressed in primary breast tumors [36, 57]. In this respect, Wip1 is the only phosphatase that shows an oncogenic property among metal-dependent serine/threonine phosphatases (the PPM family). Thus far, however, Wip1 has been reported as a relatively weak oncogene because it is not able to promote mammary tumor formation within 2 years by overexpression alone but possesses its oncogenic property in association with a cancer-initiating oncogene such as ErbB2 or myc [36, 58]. Furthermore, several pathophysiological studies have revealed that Wip1 overexpression can be a good prognostic marker for metastasis and poor survival rates in breast cancer, non-small cell lung cancer (NSCLC), and nasopharyngeal cancer patients [37, 48, 59, 60]. Conversely, the analysis of the METABRIC database performed in this study revealed that patients with Wip1 overexpression showed increased survival rates compared to patients without Wip1 overexpression in the luminal A and luminal B subtypes of breast cancer (Fig. 7b). Previously, estrogen receptor (ER)α was reported to directly bind to the Wip1 promoter as a transcription factor, and Wip1 stimulates the activity of progesterone receptor (PR) and ERα [61, 62]. As Wip1 functions as a mitotic exit phosphatase, Wip1 might be essential for ER/PR-mediated cell cycle progression in luminal A and luminal B breast cancer. Therefore, a low level of Wip1 protein in patients with the luminal A or luminal B subtype of breast cancer might be able to cause the formation of binuclear or multinuclear cells, which is one of the prognostic factors for a malignant tumor. Accordingly, Wip1 might be able to decrease the survival rate of patients with cancer by increasing genome instability as a negative regulator of the DNA damage response and increase the survival rate by maintaining faithful mitotic progression as a mitotic exit phosphatase in the context of mutations of other oncogenes and tumor progression.

Although the DNA damage response (DDR) coordinates DNA repair, cell cycle arrest, apoptosis, and senescence by activating the G1/S checkpoint and G2/M checkpoint, prolonged activation of the DDR also governs mitotic progression by regulating mitotic kinases, such as Plk1 and Aurora

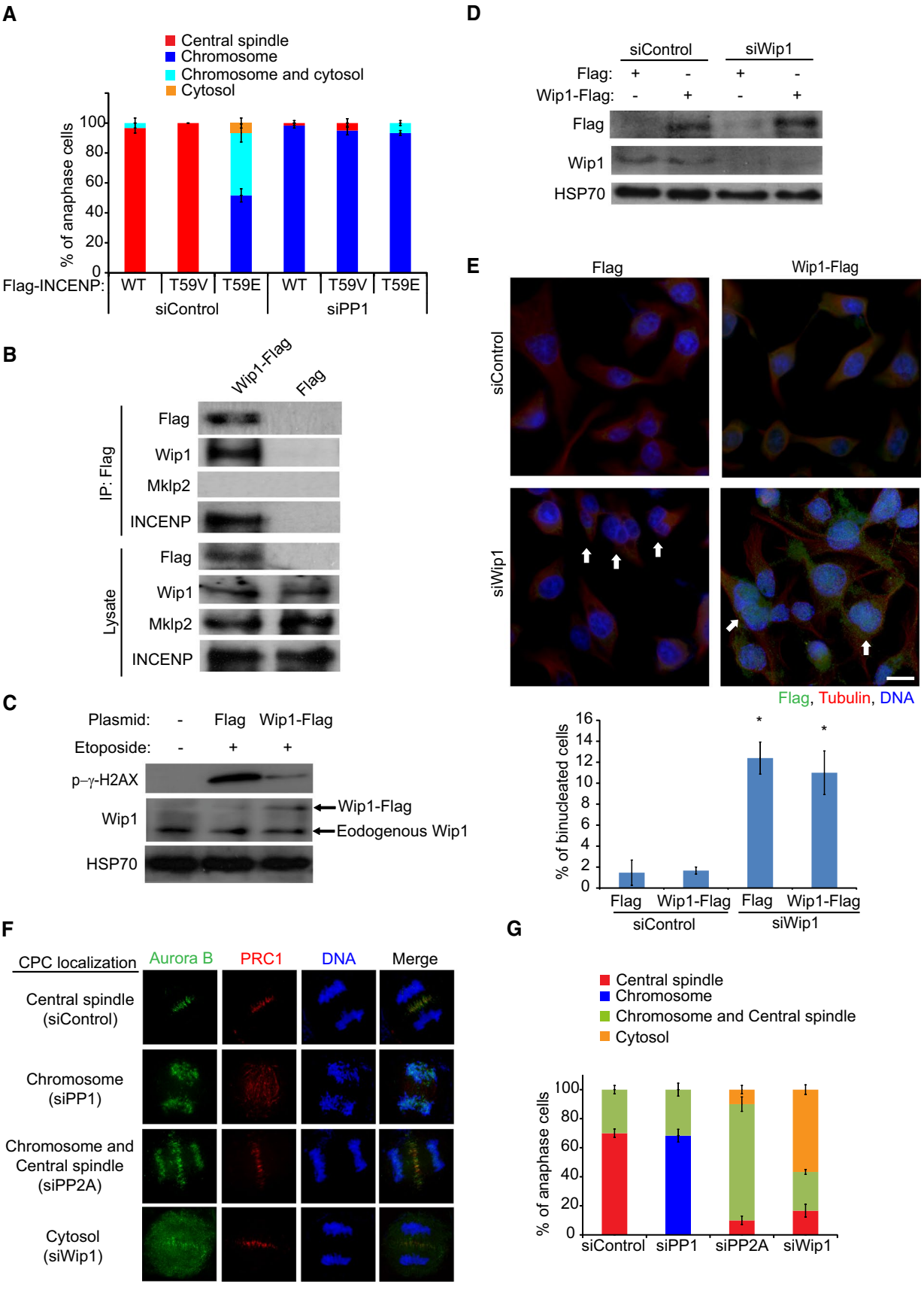
A
Central spindle
Chromosome
Chromosome and cytosol
Cytosol
% of anaphase cells
100
80
60
40
20
0
Flag-INCENP:
WT
T59V
T59E
WT
T59V
T59E
siControl
siPP1
B
Wip1-Flag
Flag
IP: Flag
Flag
Wip1
Mklp2
INCENP
Lysate
Flag
Wip1
Mklp2
INCENP
C
Plasmid: - Flag Wip1-Flag
Etoposide: - + +
p–γ-H2AX
Wip1
Wip1-Flag
Eodogenous Wip1
HSP70
D
siControl
siWip1
Flag: + - + -
Wip1-Flag: - + - +
Flag
Wip1
HSP70
E
Flag
Wip1-Flag
siControl
siWip1
Flag, Tubulin, DNA
% of binucleated cells
16
14
12
10
8
6
4
2
0
*
*
Flag
Wip1-Flag
Flag
Wip1-Flag
siControl
siWip1
F
CPC localization
Aurora B
PRC1
DNA
Merge
Central spindle (siControl)
Chromosome (siPP1)
Chromosome and Central spindle (siPP2A)
Cytosol (siWip1)
G
Central spindle
Chromosome
Chromosome and Central spindle
Cytosol
% of anaphase cells
100
80
60
40
20
0
siControl
siPP1
siPP2A
siWip1

◂**Fig. 6** Wip1 dephosphorylates INCENP at the anaphase central spindle. **a** Twenty-eight hours after the transfection of Flag-INCENP WT, the T59V mutant, or the T59E mutant, the cells were stained with antibodies against Flag and the localization of Flag-INCENP was determined from 60 anaphase cells in three independent experiments. **b** Twenty-eight hours after the transfection of Flag or Wip1-Flag WT, lysates of HeLa cells were subjected to IP followed by Western blotting. **c** Twenty-four hours after the transfection of Flag or Wip1-Flag WT, HeLa cells were treated with 10 μM etoposide. Two hours after the treatment of etoposide, the cells were harvested for Western blotting. **d**, **e** Forty-eight hours after siRNA transfection, HeLa cells were transfected with Wip1-Flag WT. Twenty-eight hours after DNA transfection, the cells were harvested for Western blotting (**d**) or stained with antibodies against Flag and tubulin (**e**). Among the cells, binucleated cells were counted in three independent experiments ($n=500$ interphase cells for each quantification). Arrows point to binucleated cells. **f**, **g** Seventy-two hours after siRNA transfection, HeLa cells were stained with antibodies against Aurora B and PRC1. The localization of Aurora B in anaphase cells was determined from 30 anaphase cells in three independent experiments. Scale bar, 20 μm. Error bars, SEM. *$p<0.01$ (two-tailed *t*-test)

B [63, 64]. Furthermore, kinases involved in the DDR, such as ATM, ATR, and Chk1, participate in mitotic processes, including Cdk1 activation in the centrosome, chromosome segregation, and cytokinesis [64–66]. Interestingly, the DDR induces mitotic catastrophe to prevent genome instability through Chk1-mediated Aurora B phosphorylation and the concomitant formation of binuclear cells through activation of abscission checkpoint and cytokinetic failure [64, 67]. In this ATR/Chk1-dependent mitotic exit DNA damage checkpoint, Wip1, a dual function phosphatase, must function as a positive regulator by dephosphorylating INCENP and concomitantly recruiting CPCs containing Aurora B to the central spindle and midbody. Concurrently, Wip1 might be able to terminate the mitotic DDR to maintain homeostasis by dephosphorylating Chk1 during mitotic exit. In this regard, Wip1 is a potential target for cancer therapy because its inhibitor might significantly inhibit the growth of breast cancer by disrupting a mitotic exit along with CPC mislocalization and sustained Chk1 activation. The molecular mechanism by which Wip1 discerns between INCENP and Chk1 in late mitosis remains to be elucidated.

In summary, we identified Wip1 as a new mitotic exit phosphatase that dephosphorylates Thr59 in INCENP for CPC translocation to the anaphase central spindle and concomitant faithful cytokinesis. Mitotic phosphatases cooperate to promote CPC translocation because PP1 detaches the CPC from mitotic chromosomes upon anaphase onset by dephosphorylating H3 at Thr3 and Wip1 dephosphorylates Thr59 in INCENP. Although Wip1 shares INCENP with PP2A as a substrate in mitotic exit, it localizes at the central spindle and acts as a major phosphatase of INCENP. Based on our novel data, Wip1 plays a role in regulating the proper progression of mitotic exit, in addition to maintaining homeostasis after the DDR. These results shed light on the mechanism by which the exquisite regulation of Wip1 activity with potential inhibitors confers new therapeutic strategies for treating cancer patients at different stages with different oncogenic mutations.

Materials and methods

Cell culture, transfection, and treatment

The human cell lines HeLa and HeLa S3 were obtained from the American Type Culture Collection (ATCC). The doxycycline-inducible WT Wip1 or DA cell lines were kindly provided by H.J. Cha, Sogang University, Seoul, Korea. All cell lines were cultured in Dulbecco's Modified Eagle's Medium (DMEM, WelGENE Inc.) supplemented with 10% fetal bovine serum (FBS, Invitrogen), penicillin (100 units/mL), and 100 μg/mL streptomycin (Invitrogen). The cells were maintained at 37 °C in a humidified atmosphere containing 5% CO_2.

siRNAs were synthesized by Genolution, Inc. (South Korea). The sequences targeting Wip1 (siWip1-A and siWip1-B) were 5′-CCAAACUUAGGAUAUAAGAUU-3′ and 5′-CCAACAUUUCUUAAAUUAUUU-3′. The sequences targeting PP1 (siPP1) were a combination of 5′-GCAUGAUUUGGAUCUUAUAUU-3′, 5′- CCGCAU CUAUGGUUUCUACUU- 3′ and 5′- UUAUGAGACCUA CUGAUGUUU- 3′. The sequences targeting PP2A (siPP2A) were a combination of 5′-GCCUAGACUUCAAUAAGA AUU-3′ and 5′-CGUCUACAGCAGUAGCAAAUU-3′. The sequence targeting Mklp2 (siMklp2) was 5′ -GAGCAAGUG GCACGUCUUCUU-3′. siRNAs were transfected into HeLa cells using DharmaFect 1 according to the manufacturer's protocol (Dharmacon, Inc.). The Flag-Wip1 WT expression plasmid was purchased from Addgene (#28105). Flag-INCENP WT, Flag-INCENP T59V, and Flag-INCENP T59E expression plasmids were kindly provided by J. Nilsson, University of Copenhagen, Copenhagen, Denmark. DNA transfection was performed using Lipofectamine 2000 according to the manufacturer's protocol (Invitrogen).

For the indicated treatments, GSK2830371 at 10 μM for 5 h (#SML1048; Sigma-Aldrich), cyclosporin A at 200 nM for 5 h (#sc-3503; Santa Cruz), calyculin A at 200 nM for 5 h (#sc-24000; Santa Cruz), and doxicycline at 0.5 μg/ml for 24 h (#sc-263109; Santa Cruz).

Western blotting, immunoprecipitation, Wip1 proteomics, and antibodies

Cells were harvested and lysed in the NP-40 lysis buffer (50 mM hepes, pH 7.4, 200 mM KCl, 0.3% NP-40, 10% glycerol, 1 mM EGTA, 1 mM $MgCl_2$, 0.5 mM DTT, 0.5 μM microcystin, 1 μg/ml pepstatin, 1 μg/ml aprotinin, 0.1 mM

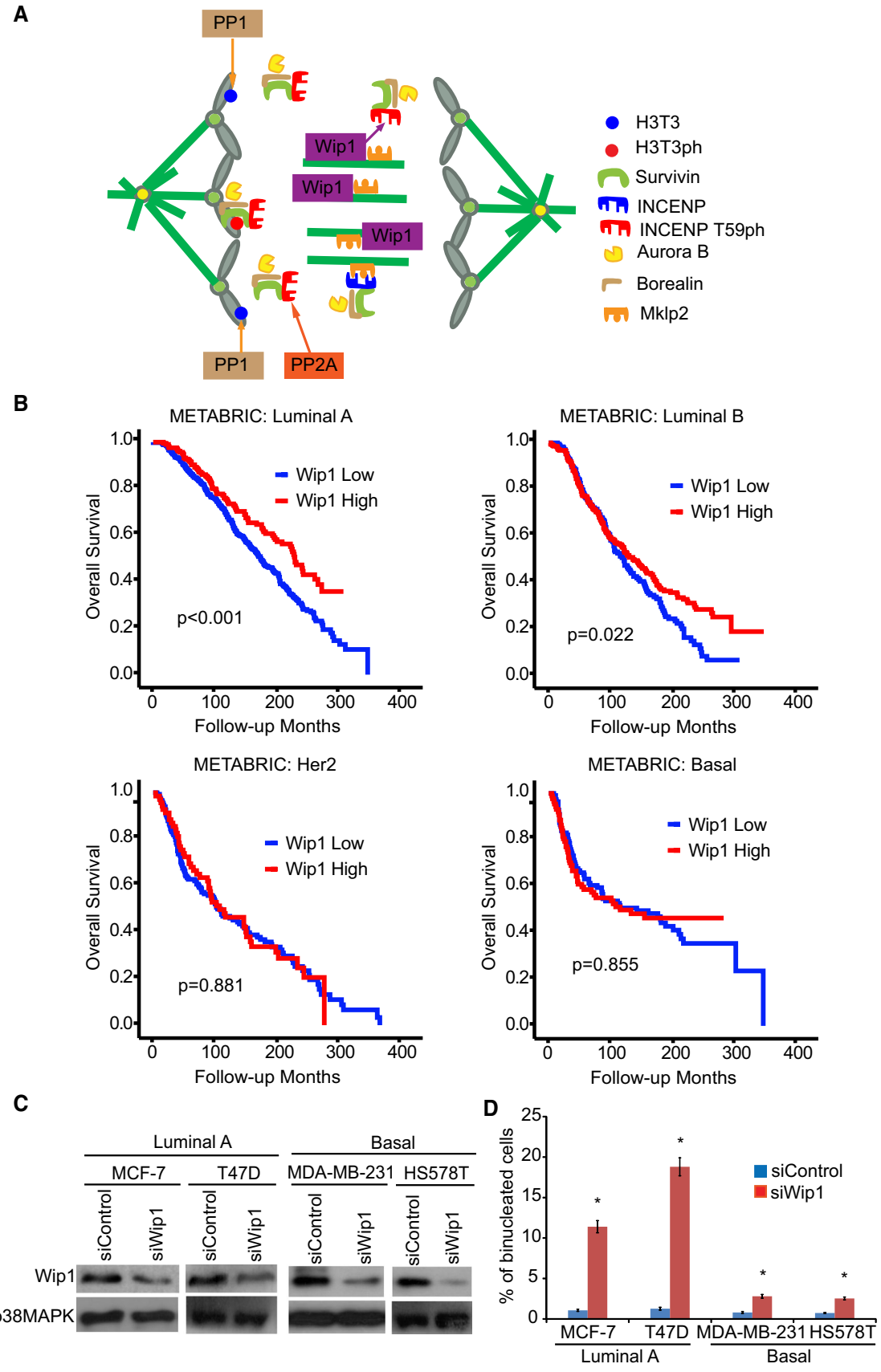
A
PP1
Wip1
Wip1
Wip1
PP1
PP2A
H3T3
H3T3ph
Survivin
INCENP
INCENP T59ph
Aurora B
Borealin
Mklp2
B
METABRIC: Luminal A
Wip1 Low
Wip1 High
p<0.001
Overall Survival
Follow-up Months
METABRIC: Luminal B
p=0.022
METABRIC: Her2
p=0.881
METABRIC: Basal
p=0.855
C
Luminal A
Basal
MCF-7
T47D
MDA-MB-231
HS578T
siControl
siWip1
Wip1
p38MAPK
D
% of binucleated cells
siControl
siWip1
MCF-7
T47D
MDA-MB-231
HS578T
Luminal A
Basal

◂**Fig. 7** Results of METABRIC data analyses. **a** Proposed model of the coordination between mitotic exit phosphatases for the translocation of CPCs from the mitotic chromosome to the central spindle in anaphase. **b** Scatter plot of Wip1 and PP2A is depicted. **c** Overall survival curves of patients stratified according to the expression of WIP1 mRNA among patients with the luminal A, luminal B, Her2, and basal subtypes of breast cancer. **d**, **e** Seventy-two hours after siRNA transfection, MCF-7, T47D, MDA-MB-231, and HS578 cells were harvested for Western blotting (**d**) or stained with antibodies against tubulin (**e**). Binucleated cells were counted in three independent experiments ($n=500$ interphase cells for each quantification). Error bars, SEM. *$p<0.01$ (two-tailed t-test)

PMSF, and 5 µg/ml leupeptin). Lysates were analyzed by SDA/PAGE using antibodies against Wip1 (#sc-37625; Santa Cruz), Hsp 90 (#sc-69703; Santa Cruze), MKLP1 (#sc-390113; Santa Cruz), MKLP2 (#H00010112-B01; Abnova), Aurora B (#ab2254; Abcam), INCENP (#ab12183; Abcam), Survivin (#ab175809; Abcam), Borealin (#NBP1-89951; Novus Biologicals), Flag (#F7425 and #F1804; Sigma-Aldrich), β-tubulin (#E7; Developmental Studies Hybridoma Bank (DSHB)), phospho-histone H3T3 (#ab78351; Abcam), phospho-histone H3S10 (#ab32107; Abcam), Cdk1 (#9116; Cell Signalling), p38 MAPK (#GTX110720; Gen Tex), PP2A-B55 alpha (#sc-81606; Santa Cruz), PP2B (#sc-365612; Santa Cruz), PP1 (#sc-7482; Santa Cruz), TPX2 (#PA3-16832; Thermo Scientific), Phospho-Aurora B T232 (#600-401-677; ROCKLAND), phospho-INCENP T59 (#12762; Signalway Antibody SAB), IgG (#ab171870; Abcam), HSP70 (#sc-32239; Santa Cruz), RhoA (#sc-418; Santa Cruz), and CHMP4A (#sc-67229; Santa Cruz).

For immunoprecipitation, indicated antibodies were coupled to Affi-Prep Protein A beads (Bio-Rad Laboratories) at a concentration of 0.3 mg/ml. Lysates were incubated with protein A beads coupled with the indicated antibodies at 4 °C overnight. Antibody beads were recovered by centrifugation, washed three times with lysis buffer in the presence of 500 mM KCl and then twice with lysis buffer, and analyzed by SDS/PAGE.

For Wip1 proteomics, the Wip1 complex was purified with beads coupled with anti-Wip1 antibodies and analyzed by liquid chromatography-tandem mass spectrometry as previously described [68].

Immunofluorescence and live-cell imaging

HeLa cells on coverslips were fixed with methanol at − 20 °C for 30 min. Alternatively, cells were extracted with BRB80-T buffer (80 mM PIPES, pH 6.8, 1 mM $MgCl_2$, 5 mM EGTA, and 0.5% Triton X-100) and then fixed with 4% paraformaldehyde for 15 min at room temperature. The fixed cells were then permeabilized and blocked with PBS-BT (1 × PBS, 3% BSA, and 0.1% Triton X-100) for 30 min at room temperature. Coverslips were then incubated in primary and secondary antibodies diluted in PBS-BT. Images were acquired using a ZEN2 (Carl Zeiss, Germany) under a Zeiss Axiovert 200 M microscope with a 1.4 NA plan-Apo 100 × oil immersion lens and an HRm CCD camera. Deconvoluted images were obtained using AutoDeblur v9.1 and AutoVisualizer v9.1 (AutoQuant Imaging). Insets show single focal planes of boxed regions.

For time-lapse microscopy, HeLa cells stably expressing GFP-H2B were cultured in Leibovitz's L-15 medium (Invitrogen) supplemented with 10% fetal bovine serum (Invitrogen) and 2 mM L-glutamine (Invitrogen). Cells were placed into a sealed growth chamber heated to 37 °C and observed on a Zeiss Axiovert 200 M microscope with a 20 × lens. Images were acquired every 3 min for 5 h with AxioVision 4.8.2 (Carl Zeiss).

Cell cycle

For cell synchronization, cells were arrested in the late G1 phase using the double thymidine block method [68]. Briefly, thymidine was added to adherent cells at a final concentration of 2 mM and the cells were cultured for 18 h. After thymidine removal and incubation for 9 h in fresh medium, thymidine was added to a final concentration of 2 mM for an additional 17 h. After thymidine removal, the synchronized cells were cultured in fresh medium and collected at different time points for cell cycle and Western blot analyses. Alternatively, the cells were synchronized in prometaphase with 16 h of nocodazole treatment and then released into fresh medium for further incubation.

For FACS analysis, cells were harvested, fixed with 70% ethanol, and stained with propidium iodide (PI) for DNA content and with phospho-MPM2 antibody for mitotic index. The cells were analyzed using FACSCalibur instrument (BD Biosciences) and FlowJo software (FLOWJO, LLC).

In vitro phosphatase assay

HeLa cells were arrested at prophase by thymidine-nocodazole treatment and then treated with Calyculin A for 5 h to inhibit the dephosphorylation of INCENP. The cells were released into fresh media for 2 h, after which the lysates were intubated with protein A agarose beads conjugated with INCENP antibody. After washing with lysis buffer three times, immunoprecipitates were incubated with GST-Wip1 (#H00008493-p01; Abnova) in phosphatase assay buffer (80 mM PIPES PH 6.8, 1 mM $Mgcl_2$, 1 mM EGTA, 1 mM DTT, 8 mM NaF, and 0.05 mM ATP) for 30 min and subjected to SDS/PAGE analysis.

METABRIC data

All METABRIC (Molecular Taxonomy of Breast Cancer International Consortium) data [69, 70] were acquired from the cBioPortal website (https://www.cbioportal.org/) with the access date of July 20th, 2018. The total number of subjects with data of Wip1 and PP2A data was 1904. The numbers of subjects with Luminal A, Luminal B, Her2, and basal subtype according to the PAM50 classification of intrinsic breast cancer subtypes [49] were 679, 461, 220, and 199, respectively. The mean follow-up interval for overall survival was 125.0 ± 76.3 months (range 0–355), and the number of subjects who died from any cause in this period was 1,103. RNA expression data were provided as the median mRNA expression value of log intensity by Illumina Human v3 microarray. The mean values of RNA expression regarding Wip1 and PP2A were 6.659 ± 0.510 (range 5.258–10.960) and 10.001 ± 0.416 (range 8.621–11.503), respectively. Subjects were classified into two groups according to RNA expression with the cutoff value as the mean value: Wip1 high group vs. Wip1 low group and PP2A high group vs. PP2A low group, respectively. The Kaplan–Meier estimator was used for survival analysis, and the log-rank test was used for comparison of survival curves between the two subject groups. The Pearson correlation coefficient (γ) was used for correlation analysis of RNA expression between Wip1 and PP2A. All statistical analyses were performed using IBM SPSS Statistics version 20.0 (IBM Inc., Armonk, NY, USA). All tests were two-sided, and a p value of 0.05 was used as the cut-off value to determine statistical significance.

Statistical analysis

Student's t-test was performed. Error bars represent the standard error (SEM) of three independent experiments, and a p value < 0.01 (two-tailed) was considered indicative of statistical significance.

Acknowledgements We thank Dr. Cha for the Wip1 inducible cell lines. We acknowledge METABRIC for generating the data. This work is supported in part by grants from the National Research Foundation of Korea (NRF-2019R1F1A1062913 and NRF-2020R1A2C1013663) and a grant from the Korea Institute of Radiological and Medical Sciences (KIRAMS) from the Ministry of Science and ICT (MSIT) of Korea (50543-2019).

Author contributions All authors contributed to project planning and data analysis of their respective experiments. CYJ and YAK coordinated the work. ZJ, JH, and JEP performed all of the biochemical experiments and imaging experiments, except analysis of the expression profile of Wip1 in the cell cycle, which was performed by EHK. KTH and YAK performed an analysis of the data obtained from the METABRIC database. All authors contributed to the writing of the paper.

Compliance with ethical standards

Conflict of interest The authors declare that they have no conflict of interest.

References

1. Stewart MP, Helenius J, Toyoda Y, Ramanathan SP, Muller DJ, Hyman AA (2011) Hydrostatic pressure and the actomyosin cortex drive mitotic cell rounding. Nature 469:226–230
2. Chircop M (2014) Rho GTPases as regulators of mitosis and cytokinesis in mammalian cells. Small GTPases 5:e29770
3. de Castro IJ, Gil RS, Ligammari L, Di Giacinto ML, Vagnarelli P (2018) CDK1 and PLK1 coordinate the disassembly and reassembly of the nuclear envelope in vertebrate mitosis. Oncotarget 9:7763–7773
4. Guttinger S, Laurell E, Kutay U (2009) Orchestrating nuclear envelope disassembly and reassembly during mitosis. Nat Rev Mol Cell Biol 10:178–191
5. Belmont AS (2006) Mitotic chromosome structure and condensation. Curr Opin Cell Biol 18:632–638
6. Walczak CE, Cai S, Khodjakov A (2010) Mechanisms of chromosome behaviour during mitosis. Nat Rev Mol Cell Biol 11:91–102
7. Bayliss R, Fry A, Haq T, Yeoh S (2012) On the molecular mechanisms of mitotic kinase activation. Open biology 2:120136
8. Domingo-Sananes MR, Kapuy O, Hunt T, Novak B (2011) Switches and latches: a biochemical tug-of-war between the kinases and phosphatases that control mitosis. Philos T R Soc B 366:3584–3594
9. Wu JQ, Guo JY, Tang W, Yang CS, Freel CD, Chen C, Nairn AC, Kornbluth S (2009) PP1-mediated dephosphorylation of phosphoproteins at mitotic exit is controlled by inhibitor-1 and PP1 phosphorylation. Nat Cell Biol 11:644-U451
10. Wurzenberger C, Gerlich DW (2011) Phosphatases: providing safe passage through mitotic exit. Nat Rev Mol Cell Bio 12:469–482
11. Errico A, Deshmukh K, Tanaka Y, Pozniakovsky A, Hunt T (2010) Identification of substrates for cyclin dependent kinases. Adv Enzyme Regul 50:375–399
12. Ubersax JA, Woodbury EL, Quang PN, Paraz M, Blethrow JD, Shah K, Shokat KM, Morgan DO (2003) Targets of the cyclin-dependent kinase Cdk1. Nature 425:859–864
13. Holt LJ, Tuch BB, Villen J, Johnson AD, Gygi SP, Morgan DO (2009) Global analysis of Cdk1 substrate phosphorylation sites provides insights into evolution. Science 325:1682–1686
14. Bouchoux C, Uhlmann F (2011) A quantitative model for ordered Cdk substrate dephosphorylation during mitotic exit. Cell 147:803–814
15. Visintin R, Craig K, Hwang ES, Prinz S, Tyers M, Amon A (1998) The phosphatase Cdc14 triggers mitotic exit by reversal of Cdk-dependent phosphorylation. Mol Cell 2:709–718
16. Stegmeier F, Amon A (2004) Closing mitosis: the functions of the Cdc14 phosphatase and its regulation. Annu Rev Genet 38:203–232
17. Queralt E, Uhlmann F (2008) Cdk-counteracting phosphatases unlock mitotic exit. Curr Opin Cell Biol 20:661–668
18. Vazquez-Novelle MD, Esteban VN, Bueno A, Sacristan MP (2005) Functional homology among human and fission yeast Cdc14 phosphatases. J Biol Chem 280:29144–29150
19. Berdougo E, Nachury MV, Jackson PK, Jallepalli PV (2008) The nucleolar phosphatase Cdc14B is dispensable for

chromosome segregation and mitotic exit in human cells. Cell Cycle 7:1184–1190
20. Mailand N, Lukas C, Kaiser BK, Jackson PK, Bartek J, Lukas J (2002) Deregulated human Cdc14A phosphatase disrupts centrosome separation and chromosome segregation. Nat Cell Biol 4:317–322
21. Bollen M, Gerlich DW, Lesage B (2009) Mitotic phosphatases: from entry guards to exit guides. Trends Cell Biol 19:531–541
22. Adams RR, Wheatley SP, Gouldsworthy AM, Kandels-Lewis SE, Carmena M, Smythe C, Gerloff DL, Earnshaw WC (2000) INCENP binds the Aurora-related kinase AIRK2 and is required to target it to chromosomes, the central spindle and cleavage furrow. Curr Biol CB 10:1075–1078
23. Kaitna S, Mendoza M, Jantsch-Plunger V, Glotzer M (2000) Incenp and an aurora-like kinase form a complex essential for chromosome segregation and efficient completion of cytokinesis. Curr Biol CB 10:1172–1181
24. Ruchaud S, Carmena M, Earnshaw WC (2007) Chromosomal passengers: conducting cell division. Nat Rev Mol Cell Biol 8:798–812
25. Wilkins BJ, Rall NA, Ostwal Y, Kruitwagen T, Hiragami-Hamada K, Winkler M, Barral Y, Fischle W, Neumann H (2014) A cascade of histone modifications induces chromatin condensation in mitosis. Science 343:77–80
26. Kim S, Kim NH, Park JE, Hwang JW, Myung N, Hwang KT, Kim YA, Jang CY, Kim YK (2020) PRMT6-mediated H3R2me2a guides Aurora B to chromosome arms for proper chromosome segregation. Nat Commun 11:612
27. Kelly AE, Ghenoiu C, Xue JZ, Zierhut C, Kimura H, Funabiki H (2010) Survivin reads phosphorylated histone H3 threonine 3 to activate the mitotic kinase Aurora B. Science 330:235–239
28. Liu D, Vader G, Vromans MJ, Lampson MA, Lens SM (2009) Sensing chromosome bi-orientation by spatial separation of aurora B kinase from kinetochore substrates. Science 323:1350–1353
29. Carmena M, Wheelock M, Funabiki H, Earnshaw WC (2012) The chromosomal passenger complex (CPC): from easy rider to the godfather of mitosis. Nat Rev Mol Cell Biol 13:789–803
30. Hummer S, Mayer TU (2009a) Cdk1 negatively regulates midzone localization of the mitotic kinesin Mklp2 and the chromosomal passenger complex. Curr Biol CB 19:607–612
31. Hein JB, Hertz EPT, Garvanska DH, Kruse T, Nilsson J (2017) Distinct kinetics of serine and threonine dephosphorylation are essential for mitosis. Nat Cell Biol 19:1433–1440
32. van der Horst A, Lens SM (2014) Cell division: control of the chromosomal passenger complex in time and space. Chromosoma 123:25–42
33. van der Waal MS, Hengeveld RC, van der Horst A, Lens SM (2012) Cell division control by the chromosomal passenger complex. Exp Cell Res 318:1407–1420
34. Fiscella M, Zhang H, Fan S, Sakaguchi K, Shen S, Mercer WE, Vande Woude GF, O'Connor PM, Appella E (1997) Wip1, a novel human protein phosphatase that is induced in response to ionizing radiation in a p53-dependent manner. Proc Natl Acad Sci USA 94:6048–6053
35. Lu X, Nannenga B, Donehower LA (2005) PPM1D dephosphorylates Chk1 and p53 and abrogates cell cycle checkpoints. Genes Dev 19:1162–1174
36. Bulavin DV, Demidov ON, Saito S, Kauraniemi P, Phillips C, Amundson SA, Ambrosino C, Sauter G, Nebreda AR, Anderson CW et al (2002) Amplification of PPM1D in human tumors abrogates p53 tumor-suppressor activity. Nat Genet 31:210–215
37. Rauta J, Alarmo EL, Kauraniemi P, Karhu R, Kuukasjarvi T, Kallioniemi A (2006) The serine-threonine protein phosphatase PPM1D is frequently activated through amplification in aggressive primary breast tumours. Breast Cancer Res Tr 95:257–263
38. Jeong HC, Gil NY, Lee HS, Cho SJ, Kim K, Chun KH, Cho H, Cha HJ (2015) Timely degradation of Wip1 phosphatase by APC/C activator protein Cdh1 is necessary for normal mitotic progression. J Cell Biochem 116:1602–1612
39. Macurek L, Benada J, Mullers E, Halim VA, Krejcikova K, Burdova K, Pechackova S, Hodny Z, Lindqvist A, Medema RH et al (2013) Downregulation of Wip1 phosphatase modulates the cellular threshold of DNA damage signaling in mitosis. Cell Cycle 12:251–262
40. Horn V, Thelu J, Garcia A, Albiges-Rizo C, Block MR, Viallet J (2007) Functional interaction of Aurora-A and PP2A during mitosis. Mol Biol Cell 18:1233–1241
41. Andreassen PR, Lacroix FB, Villa-Moruzzi E, Margolis RL (1998) Differential subcellular localization of protein phosphatase-1 alpha, gamma1, and delta isoforms during both interphase and mitosis in mammalian cells. J Cell Biol 141:1207–1215
42. Bulavin DV, Phillips C, Nannenga B, Timofeev O, Donehower LA, Anderson CW, Appella E, Fornace AJ (2004) Inactivation of the Wip1 phosphatase inhibits mammary tumorigenesis through p38 MAPK-mediated activation of the p16(Ink4a)-p19(Arf) pathway. Nat Genet 36:343–350
43. Cha H, Lowe JM, Li H, Lee JS, Belova GI, Bulavin DV, Fornace AJ Jr (2010) Wip1 directly dephosphorylates gamma-H2AX and attenuates the DNA damage response. Cancer Res 70:4112–4122
44. Takekawa M, Adachi M, Nakahata A, Nakayama I, Itoh F, Tsukuda H, Taya Y, Imai K (2000) p53-inducible wip1 phosphatase mediates a negative feedback regulation of p38 MAPK-p53 signaling in response to UV radiation. EMBO J 19:6517–6526
45. Goto H, Kiyono T, Tomono Y, Kawajiri A, Urano T, Furukawa K, Nigg EA, Inagaki M (2006) Complex formation of Plk1 and INCENP required for metaphase-anaphase transition. Nat Cell Biol 8:180-U152
46. Hummer S, Mayer TU (2009b) Cdk1 negatively regulates midzone localization of the mitotic kinesin Mklp2 and the chromosomal passenger complex. Curr Biol 19:607–612
47. Qian JB, Lesage B, Beullens M, Van Eynde A, Bollen M (2011) PP1/repo-man dephosphorylates mitotic histone H3 at T3 and regulates chromosomal aurora B targeting. Curr Biol 21:766–773
48. Zhao M, Zhang HB, Zhu GY, Liang J, Chen N, Yang YH, Liang XC, Cai HM, Liu W (2016) Association between overexpression of Wip1 and prognosis of patients with non-small cell lung cancer. Oncol Lett 11:2365–2370
49. Parker JS, Mullins M, Cheang MCU, Leung S, Voduc D, Vickery T, Davies S, Fauron C, He XP, Hu ZY et al (2009) Supervised risk predictor of breast cancer based on intrinsic subtypes. J Clin Oncol 27:1160–1167
50. Grallert A, Boke E, Hagting A, Hodgson B, Connolly Y, Griffiths JR, Smith DL, Pines J, Hagan IM (2015) A PP1-PP2A phosphatase relay controls mitotic progression. Nature 517:94–98
51. Mochida S, Hunt T (2012) Protein phosphatases and their regulation in the control of mitosis. Embo Rep 13:197–203
52. Olsen JV, Vermeulen M, Santamaria A, Kumar C, Miller ML, Jensen LJ, Gnad F, Cox J, Jensen TS, Nigg EA et al (2010) Quantitative phosphoproteomics reveals widespread full phosphorylation site occupancy during mitosis. Sci Signal 3:3
53. Qian JB, Winkler C, Bollen M (2013) 4D-networking by mitotic phosphatases. Curr Opin Cell Biol 25:697–703
54. Hara M, Abe Y, Tanaka T, Yamamoto T, Okumura E, Kishimoto T (2012) Greatwall kinase and cyclin B-Cdk1 are both critical constituents of M-phase-promoting factor. Nat Commun 3:1059
55. Rossio V, Yoshida S (2011) Spatial regulation of Cdc55-PP2A by Zds1/Zds2 controls mitotic entry and mitotic exit in budding yeast. J Cell Biol 193:445–454
56. Yu E, Ahn YS, Jang SJ, Kim MJ, Yoon HS, Gong G, Choi J (2007) Overexpression of the wip1 gene abrogates the p38 MAPK/p53/

Wip1 pathway and silences p16 expression in human breast cancers. Breast Cancer Res Treat 101:269–278
57. Li J, Yang Y, Peng Y, Austin RJ, van Eyndhoven G, Nguyen KCQ, Gabriele T, McCurrach ME, Marks JR, Hoey T et al (2002) Oncogenic properties of PPM1D located within a breast cancer amplification epicenter at 17q23. Nat Genet 31:133–134
58. Demidov ON, Kek C, Shreeram S, Timofeev O, Fornace AJ, Appella E, Bulavin DV (2007) The role of the MKK6/p38 MAPK pathway in Wip1-dependent regulation of ErbB2-driven mammary gland tumorigenesis. Oncogene 26:2502–2506
59. Canevari RA, Marchi FA, Domingues MAC, de Andrade VP, Caldeira JRF, Verjovski-Almeida S, Rogatto SR, Reis EM (2016) Identification of novel biomarkers associated with poor patient outcomes in invasive breast carcinoma. Tumor Biol 37:13855–13870
60. Sun GG, Zhang J, Ma XB, Wang YD, Cheng YJ, Hu WN (2015) Overexpression of wild-type p53-induced phosphatase 1 confers poor prognosis of patients with nasopharyngeal carcinoma. Pathol Oncol Res 21:283–291
61. Proia DA, Nannenga BW, Donehower LA, Weigel NL (2006) Dual roles for the phosphatase PPM1D in regulating progesterone receptor function. J Biol Chem 281:7089–7101
62. Han HS, Yu E, Song JY, Park JY, Jang SJ, Choi J (2009) The estrogen receptor alpha pathway induces oncogenic Wip1 phosphatase gene expression. Mol Cancer Res MCR 7:713–723
63. Lee HJ, Hwang HI, Jang YJ (2010) Mitotic DNA damage response: polo-like kinase-1 is dephosphorylated through ATM-Chk1 pathway. Cell Cycle 9:2389–2398
64. Mackay DR, Ullman KS (2015) ATR and a Chk1-Aurora B pathway coordinate postmitotic genome surveillance with cytokinetic abscission. Mol Biol Cell 26:2217–2226
65. Kramer A, Mailand N, Lukas C, Syljuasen RG, Wilkinson CJ, Nigg EA, Bartek J, Lukas J (2004) Centrosome-associated Chk1 prevents premature activation of cyclin-B-Cdk1 kinase. Nat Cell Biol 6:884–891
66. Kabeche L, Nguyen HD, Buisson R, Zou L (2018) A mitosis-specific and R loop-driven ATR pathway promotes faithful chromosome segregation. Science 359:108–114
67. Huang XX, Tran T, Zhang LN, Hatcher R, Zhang PM (2005) DNA damage-induced mitotic catastrophe is mediated by the Chk1-dependent mitotic exit DNA damage checkpoint. Proc Natl Acad Sci USA 102:1065–1070
68. Jang CY, Wong J, Coppinger JA, Seki A, Yates JR, Fang GW (2008) DDA3 recruits microtubule depolymerase Kif2a to spindle poles and controls spindle dynamics and mitotic chromosome movement. J Cell Biol 181:255–267
69. Curtis C, Shah SP, Chin SF, Turashvili G, Rueda OM, Dunning MJ, Speed D, Lynch AG, Samarajiwa S, Yuan Y et al (2012) The genomic and transcriptomic architecture of 2,000 breast tumours reveals novel subgroups. Nature 486:346–352
70. Pereira B, Chin SF, Rueda OM, Vollan HKM, Provenzano E, Bardwell HA, Pugh M, Jones L, Russell R, Sammut SJ et al (2016) The somatic mutation profiles of 2,433 breast cancers refines their genomic and transcriptomic landscapes. Nat Commun 7:11479